Chemical Kinetic Modelling Study on the Influence of *n*-butanol blending on the Combustion, Autoignition and Knock Properties of Gasoline and its Surrogate in a Spark Ignition Engine.

E. Agbro[1], A. S. Tomlin[1], W. Zhang[2] A. Burluka[3], F. Mauss[4], M. Pasternak[4], A. Alfazazi[5], S.M Sarathy[5]

[1]School of Chemical and Process Engineering, University of Leeds, Leeds, UK.
[2]School of Mechanical Engineering, University of Leeds, Leeds, UK
[3]Faculty of Engineering and Environment, Northumbria University, Newcastle, UK.
[4]Department of Thermodynamics and Thermal Process Engineering, Brandenburg University of Technology, Cottbus, Germany.
[5]King Abdullah University of Science and Technology, Clean Combustion Research Center, Thuwal, Saudi Arabia

Abstract

The ability of a mechanism describing the oxidation kinetics of toluene reference fuel (TRF)/*n*-butanol mixtures to predict the impact of *n*-butanol blending at 20% by volume on the autoignition and knock properties of gasoline has been investigated under conditions of a strongly supercharged spark ignition (SI) engine. Simulations were performed using the LOGEengine code for stoichiometric fuel/air mixtures at intake temperature and pressure conditions of 320 K and 1.6 bar, respectively, for a range of spark timings.

At the later spark timing of 6 °CA bTDC, the predicted knock onsets for a gasoline surrogate (toluene reference fuel, TRF) and the TRF/*n*-butanol blend are higher compared to the measurements, which is consistent with an earlier study of ignition delay times predicted in a rapid compression machine (RCM, Agbro et al., Fuel, 2017, 187:211-219). The discrepancy between the predicted and measured knock onsets is however quite small at higher pressure and temperature conditions (spark timing of 8 °CA bTDC) and can be improved by updating a key reaction related to the toluene chemistry. The ability of the scheme to predict the influence of *n*-butanol blending on knock onsets requires improvement at later spark timings. The simulations highlighted that the low-intermediate temperature chemistry within the SI engine end gas, represented by the presence of a cool flame and negative temperature coefficient (NTC) phase, plays an important role in influencing the high temperature heat release and consequently the overall knock onset. This is due to its sensitisation effect (increasing of temperature and pressure) on the end gas and reduction of the time required for the high temperature heat release to occur. Therefore, accurate representation of the low-intermediate temperature chemistry is crucial for predicting knock. The engine simulations

provide temperature, heat release and species profiles that link conditions in practical devices and ignition delay times predicted in an RCM. This facilitates a better understanding of the chemical processes affecting knock onsets predicted within the engine and the main reactions governing them.

Keywords: *n*-butanol, autoignition, spark ignition engine, modelling.

1.0 Introduction

Engine downsizing, aimed at reducing the engine swept volume and consequently fuel consumption without penalising power output, is currently considered as a viable strategy in the automotive industry for improving the efficiency of gasoline engines. In order for a downsized engine to achieve the same amount of power as the original engine, a boosting system (supercharging) is usually required to increase the density of inlet air. However, supercharging and the use of high compression ratios are currently limited by the phenomena of knock.[1] This leads to an increased demand for fuels with high anti-knock qualities as blending agents (i.e., octane enhancers)[2] and has triggered a renewed interest in better understanding the autoignition and knock performance of alternative fuels, such as biofuels, when blended with gasoline for the purpose of optimising engine design and control strategies such as ignition timing optimisation. The wider penetration and optimal use of biofuels and their blends with gasoline in spark ignition (SI) engines requires a thorough understanding of their autoignition and knock behaviour under a wide range of conditions and this could be most efficiently realised through computer modelling and analysis. Autoignition and knock in an engine are governed by chemical kinetics and depend on the chemical composition of the fuel and on the evolution of pressure, temperature and equivalence ratio.[1] It would therefore be helpful to be able to use computer simulations employing kinetic mechanisms of fuels in main engine combustion models to reliably predict and understand autoignition and consequently the knocking of alternative fuel blends in engines.

Previously, attempts have been made to predict autoignition using various simple empirical models. Two such correlations are the popular Douaud and Eyzat (D&E) model[3] derived from the Arrhenius function, and the Livengood-Wu integral.[4] In terms of chemical kinetic modelling, the prediction of autoignition in engines has predominantly been limited to the use of global chemical reaction mechanisms developed for a limited number of fuels, such the

'Shell model'[5] comprising 5 species and 8 generalised reactions representing chain/degenerate branching and termination steps, and the skeletal Hu and Keck model.[6] However these global kinetic models, just like the empirical models, have been proven to be inaccurate in terms of agreement with measured data for predictions of practical combustors. The various unique features of low temperature combustion such as cool flames and two stage ignition as well as the long ignition delay times exhibited by certain hydrocarbon fuels can only be reasonably explained by including intermediate elementary reactions that make up detailed reaction mechanisms. Therefore, the use of detailed or specifically reduced reaction mechanisms coupled to main engine combustion models offers a greater capability to predict autoignition in engines, and therefore forms the basis for this study.

It should be noted however, that kinetic models are generally developed and validated within the framework of fundamental setups such as rapid compression machines (RCMs), jet stirred reactors (JSRs), shock tubes etc., where the effects of fluid dynamics and turbulence are suppressed.[7-9] A recent RCM ignition delay study of Agbro et al.[10], for example, suggested that blending *n*-butanol to 20% by volume with a reference gasoline and a formulated surrogate led to increased delays at temperatures below 800 K but shorter ignition delays at higher temperatures. The detailed version of the kinetic mechanism employed in the present study was able to capture these effects. However, this means that the region where *n*-butanol may act as an octane enhancer existed where the prevailing pressure-temperature (*P*-*T*) conditions are likely to be more representative of the *P*-*T* conditions occurring before autoignition in homogeneous compression charged ignition (HCCI) and/or controlled autoignition (CAI) engines rather than in SI engines. Therefore it crucial to test the effects of blending, as well as our ability to model blending effects, under supercharged SI engine conditions.

Although a limited number of detailed and reduced chemical kinetic models of alternative fuels for bio-butanols[11-18] and their blends with conventional gasoline surrogate fuels[19] have been developed for use within the context of engine simulations, these models have been rarely applied or investigated under real engine conditions where the effects of fluid dynamics, high variable pressures and temperatures, as well as variable volume combustion and flame propagation are accounted for. A notable exception is the recent HCCI modelling study of Pelucchi et al.[20] for higher alcohols, although in their study a homogeneously mixed multi-zone engine model was used to reduce computing time. Thus, one novel aspect of this

study is to extend the use of detailed chemical models of fuel blends to more realistic engine simulations using stochastic reactor models. A particular objective is to assess the ability of a reduced toluene reference fuel (TRF)/*n*-butanol blended mechanism, based on that presented in Agbro et al.,[10] to accurately predict the autoignition and knock behaviour of gasoline and a gasoline/*n*-butanol blend under practical SI engine conditions, using a stochastic approach. Moreover, there is a need to link our current fundamental kinetic understanding of alternative fuels with their performance in real engines conditions. Thus a further objective of the study is to link the fundamental understanding developed from the chemical kinetic modelling of autoignition within an RCM as presented in previous work,[10] with the performance of a reduced version of the TRF/*n*-butanol scheme in predicting autoignition and knock within a supercharged SI engine. This will allow us to evaluate whether simpler set-ups such as RCMs are useful tests of the validity of kinetic models for their subsequent use in practical engine design applications.

2.0 Methodology

2.1 Chemical kinetic scheme

There is a consensus that autoignition of the end gas in SI engines is mainly driven by the fuel oxidation chemistry[21], which in turn is influenced by the engine operating parameters (*T*/*P*) and factors affecting the fluid dynamics of the reactive system (e.g. combustion chamber, intake valve and exhaust valve design). The awareness of the role of chemical kinetics in the numerical prediction of knock in practical engines has sparked great interest in the development of chemical kinetic models of fuel oxidation. The simplest and most basic form of chemical kinetic models that have been used for modelling of the end gas autoignition in engines are global chemical kinetic models such as developed by Hu and Keck[6] based on earlier work by Cox and Cole[22] and Benson.[23] Extended versions of the Hu and Keck mechanisms,[24-26] generally referred to as the Skeletal Keck mechanisms were however shown in[9] to display significant discrepancies with measurements in terms of their autoignition predictions when compared to both detailed[27] and reduced[28-30] versions of the Lawrence Livermore National Laboratory (LLNL) mechanisms for primary reference fuel (PRF).

While a few detailed and reduced mechanisms of gasoline oxidation exist currently in the literature,[19] the only combined oxidation mechanism for TRF (toluene, n-heptane, iso-octane mixture)/*n*-butanol blends available at the time of this study was the detailed scheme presented in Agbro et al.[10] For the purpose of this study, a reduced TRF/*n*-butanol blended mechanism was developed from the detailed scheme for use in the context of simulating autoignition and knock in the engine. The detailed scheme contains 1944 species and 8231 elementary reactions while the reduced scheme employed here is comprised of 527 species and 2644 reaction steps. More information on the detailed TRF/*n*-butanol blended mechanism can be found in ref.[10] Model reduction was carried out using the method of direct relation graph with expert knowledge, DRG-X.[31] The model was reduced for low temperatures (600-950 K), and a range of pressures from 1-20 bar, with a fractional error for heat release set at 0.03. The reduced mechanism was tested by comparing predicted ignition delays against those from the full mechanism for the different mixtures across a range of temperatures and pressures up to 50 bar, with very small resulting differences. Both the mechanism, as well as comparisons of predicted ignition delay times between the full and reduced schemes, performed in zero dimensional, non-stochastic, simulations, are available in the Supplementary Material of this paper. The model reduction and the resulting validation comparisons were carried out for the blends.

2.2 Supporting Experiments

The supporting experiments used for the modelling study are fully described in a companion paper within this volume. However brief details are given here for completeness. The experiments were conducted in the Leeds University Ported Optical Engine, Mk II, with a Disc-shaped combustion chamber and central ignition.[32] This engine has a port arrangement which minimises charge flow non-uniformities, thus allowing accurate control of air and fuel pressure, temperature and flow rates. In order to avoid dilution with trapped residual exhaust gases, the engine is operated in a skip-firing mode with the cylinder flushed with fresh mixture during the cycles with skipped ignition; typically only one in 20 cycles was fired. The in-cylinder pressure was measured with piezoelectric pressure transducers and the onset of autoignition was determined as the appearance of an inflection point in the pressure signal when passed through low-pass filter.[33] Throughout the experiments, LUPOE-2D was operated at a speed of 750 RPM at an initial charge temperature of 323 K, intake pressure of 1.6 bar and an equivalence ratio of 1. A total of four fuel mixtures were tested experimentally: a

reference commercial gasoline of research octane number (RON) 95 referred to as ULG, a toluene reference fuel (TRF), a blend of 20 % by volume of *n*-butanol with 80 % by volume of RON95 gasoline (ULGB20) and a blend of 20 % by volume of *n*-butanol with 80 % by volume of TRF (TRFB20).[10]

2.3 Modelling

The chemical kinetic modelling of knock onsets of the gasoline and gasoline/*n*-butanol blend in the Leeds engine setup was carried out within the LOGEengine simulation platform using the stochastic reactor model (SRM) with turbulent flame propagation (TFP).[34] The reduced version of the TRF/*n*-butanol blended reaction mechanism presented in ref[10] which was based on the original butanol scheme of Sarathy[13] was used as input in the engine simulations for the prediction of the knock onsets of the various fuel mixtures. The SRM is a 0D model of physical and chemical processes occurring in combustion engines during the closed part of the engine cycle. For SI engines, the SRM is formulated as a two-zone model in which the burned and unburned zones are separated by a spherical flame propagating across the combustion chamber. The SRM is a probability based model and simulates the in-cylinder mixture (both the burned and unburned zones) as an ensemble of particles which are capable of exchanging heat and mass among themselves within a zone. Each zone is assumed to be statistically homogenous, and particle-particle interaction is purely stochastic. Each particle has a chemical composition, temperature and mass, and hence, each particle represents a point in phase-space for species mass fraction and temperature. Mixing time is the main modelled parameter for the SRM. By its modelling, inhomogeneity is introduced into the gas-phase for species concentration and temperature. Besides the impact of mixing, the mixture inhomogeneity is further enhanced by the heat transfer to the wall and fuel injection. Overall, the modelled inhomogeneity of the mixture mimics, to a reasonable extent, the turbulence effects in actual engines.

The LOGEengine software comes with an optimisation tool which incorporates an inbuilt initial condition calibration tool and a mixing time optimisation tool. Initial condition calibration involves the analysis of experimental data through an extended heat release analysis, which additionally helps to eliminate possible inaccuracies present in the measurement. Given an engine geometry and measured pressure trace, the LOGEengine determines the initial conditions such as initial mass, temperature, mixture composition, internal EGR and absolute pressure as outlined in Table 1. Following the heat release

analysis, the data is exported to the mixing time optimisation tool where a full scale simulation is performed with detailed chemistry, optimising against, for example, indicated mean effective pressure or engine exhaust emissions, with pressure used in this study. Both the initial condition calibration tool and the mixing time optimisation tool make use of genetic algorithms in order to find the best simulation setup and match for any given case. In the optimisation or calibration process, the experimental and simulated in-cylinder pressure traces during the combustion phase are effectively matched through the tuning of the mixing time. The temperature history of the end gas ahead of the spark-initiated flame is then also taken to be reasonably matched. With this in place, the influence of chemical processes can then be decoupled from the impact of all other factors such as turbulent flame propagation and variations in *P-T* conditions. Autoignition and knock in an SI engine originates from the unburned zone as a result of end gas compression by the propagating flame and is governed mainly by the chemical kinetics of the fuel. Therefore the predicted autoignition onset (knock onset) is detected in LOGEengine by analysis of the unburned zone heat release and species concentration profiles. Knock onset is predicted at the point of significant heat release rate[21] which also coincides with a rapid increase in the OH radical concentration as well as a decrease in the concentration of CH_2O as will be shown in the later results section. It is important to state that while autoignition is the primary process for the development towards knocking combustion, sometimes it does not give rise to knock. In Pasternak et al. [35, 36] the strong second peak in the unburned zone rate of heat release profile (RoHR-u) was linked with the occurrence of knock. Validity of this simplified identification of knock onset has to some extent been confirmed by the results presented in Pasternak et al.[35] but this assumption is still only approximate. Since the experimental and simulated pressure profile and consequently temperature history have been matched for the combustion phase, any differences between the predicted and measured autoignition onset are solely dependent on the specific chemical kinetic model employed. The various engine design and engine operating parameters used for the calibration process are shown in Table 1.

Table 1: Basic input for SI engine calculations: [a]Parameter required in the Woshni heat transfer correlation for the calculation of wall heat transfer.

Simulation parameters	
Engine parameters	
SPEED	750 RPM

BORE	0.08 (m)
COMPRESSION RATIO	11.5
STROKE	0.110 (m)
ROD LENGTH	0.232 (m)
Amount of Exhaust Gas Recirculation (EGR)	3 %
Number of EGR cycles	1
Heat Transfer parameters	
Wall temperature	450 (K)
Woshni_AP0[a]	1.370
Initial conditions	
Temperature	323 (K)
Pressure	0.16 x 10^6 (N/m^2)

2.2.1 Flame propagation model

The present work used a quasi-3D turbulent flame propagation (TFP) model for determining the mass burn rate. This model assumes that the flame is spherically expanding and is truncated by the cylinder walls. The turbulent flame speed S_T is derived from the turbulence root-mean-square (rms) velocity u' and the laminar flame speed S_L using the correlation of Peters[36, 37] given by:

$$\frac{S_T}{S_L}=1+C\left(\frac{u'}{S_L}\right)^n ; 0.5<n<1 \quad (1)$$

where n and C are adjustable constants with n ranging from 0.5-1.0.[36, 38]

Since there are no available measurements available for the blends studied here, the laminar flame speed S_L is obtained using the default laminar flame speed library for pure iso-octane[39], covering the wide range of conditions (temperatures, pressures, equivalence ratios and exhaust gas recirculation (EGR) rates). During simulations, the specific value of the flame speed required under a set of conditions is retrieved more quickly with the help of an advanced correlation function implemented in LOGEengine. Because the emphasis here is on the investigation of the pre-flame chemistry, the model for the flame propagation only needs to reproduce the pressure and temperature history driving the auto-ignition. Furthermore, because of the optimisation process within LOGEengine, the important parameters such as mixing time-scales are informed by the experimental pressure profiles and hence are not very sensitive to the input laminar flame speeds. In this work, all engine computations were performed using the default values of C = 2.5 and n = 0.9 in order to keep the complexity of

the simulation process to a minimum. The root mean square velocity u' is calculated using the relation,

$$u' = \frac{l}{\tau_t} \quad (2)$$

where l_I is the integral length scale of the flow and τ_t is the turbulent mixing time; both variables are modified in this work so as to fit the calculated pressure trace to the measured one. The rms velocity fluctuation is a good indicator of the level of turbulence in the engine. The time evolution of the integral length scale is only slightly dependent on the engine operation.[9] Therefore a constant value of l = 0.04 m was used in the calculation of u', somewhat larger than the measured values. [40, 41]

The TFP model gives a better representation of the effect of engine geometry and operating conditions on combustion compared to the Wiebe function. The turbulent intensity or turbulent mixing time helps to account for the physical process of turbulent mixing which is a function of engine geometry. The laminar flame velocity, used in computing the turbulent flame velocity, is determined as a function of engine operating conditions such as pressure and temperature. The fuel effect (chemistry effect) is modelled by the chemical kinetic mechanism employed in the simulations. A full description of the engine set-up and experimental methodology is given in the companion paper which precedes this work in the special issue.

3.0 Results and discussions

3.1 Simulations and comparison with experimental data

The overall aim of this work is to investigate fuel chemistry effects on autoignition and knocking within the LUPOE. Therefore, it is important to ensure that there are no significant differences between the thermodynamic state of the simulated and experimental conditions across the set of fuels being compared so that the end gas is subject to the same *P-T* history across all fuels. According to Khan[9] and in line with the findings of Materego[42], the heat loss characteristics of the fuels under consideration are not significantly affected by the fuel composition as they exhibit very similar heat loss profiles under the same pre-knock *P-T* conditions. A multi-zone RCM modelling study by Ahmed at al.[43] did note some differences

in ignition delay times due to heat losses from different surrogate fuel formulations but these were found to be less significant in the intermediate temperature region around the NTC. Matching the in-cylinder pressure across the fuels, should largely result in a match of the pre-knock temperature history of the end gas ahead of the propagating flame. Similar to the approach employed in Khan[9], the mean experimental pressure cycle of the reference gasoline was selected and matched across spark timings of 6 °CA, 7 °CA and 8 °CA. This approach was mainly employed since a cycle-by-cycle comparison across all fuels is not possible due to the different levels of cyclic variability exhibited by all the fuels tested as shown in the companion experimental paper. Therefore, the mean pressure cycle of the reference gasoline, which is representative of the *P-T* conditions across all four fuels at a particular spark timing, was employed for calibration of initial engine conditions required as input in the engine simulations. Across the four fuels (ULG, TRF, ULGB20 and TRFB20), experimental pressure cycles with pre-knock values very close to the mean pressure cycle of the reference gasoline were then selected for knock onset averaging . The estimated average knock onsets of the selected cycles for ULG, TRF, ULGB20 and TRFB20 presented in Figure 1 are considered here as representative of the overall average across the respective fuels.

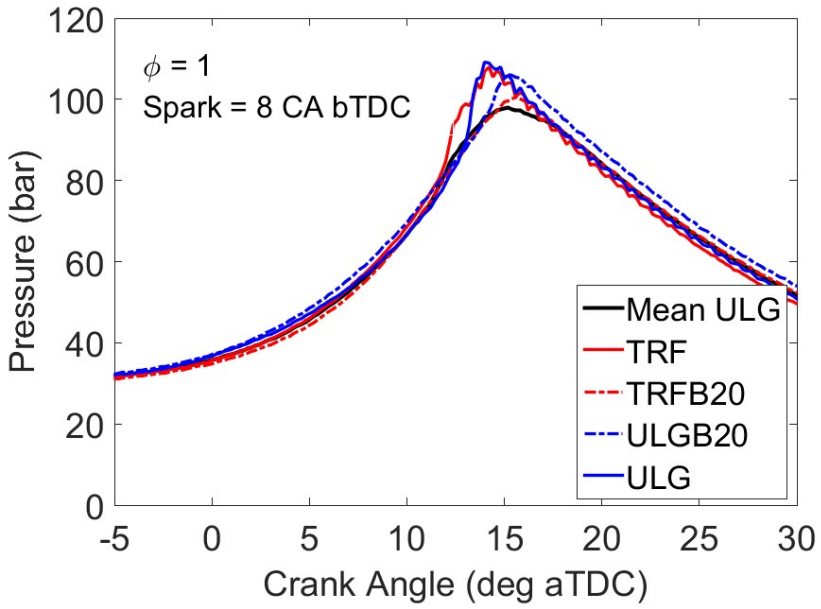

Figure 1. Selected experimental pressure cycles of four fuels with pre-knock values close to that of the mean cycle for gasoline.

3.1.1 Prediction of the average knocking combustion properties of gasoline

Figure 2 shows a comparison of the experimental pressure trace and the simulated pressure trace for TRF at an intake temperature and pressure of 320 K and 1.6 bar respectively at spark timings of 6 and 8 °CA bTDC. As shown in Figures 2a and 2b, the simulated pressure traces are in reasonably good agreement with the measured pressure traces, with a better match being achieved for the spark timing of 8 °CA bTDC. The small discrepancy between the optimised pressure in the simulations and the measured pressure at around 10 °CA bTDC for the spark timing of 6 °CA bTDC may also impact on the simulated temperatures, and thus the reaction rates of the low temperature chemistry. However, estimated heat release rates (HRR) were well matched for all conditions. HRR were not directly measured within the experiments but can be derived from the measured pressure traces. Comparisons between the simulated and experimentally derived HRR for different blends and spark timings are also shown in Supplementary Material and following the optimisation process are seen to match very well. The level of agreement was obtained with an optimised turbulence mixing time of 0.022 s and an integral length scale of 0.04 m. A small EGR of 3 % was employed in all simulations in order to represent any trapped residuals based on the assumption that the combustion chamber is largely free of exhaust products due to the high skip firing ratio employed in the experiments. The deviation between the measured and simulated pressure traces during the expansion phase after around 35 °CA aTDC can be explained on the basis of the approximated cylinder profile and spark plug position employed in the simulation. There is also a slight discrepancy during the compression phase, which suggests that given the assumed geometric parameters of the combustion chamber and the flame shape of a truncated sphere, a perfect optimisation could not be achieved. Since the simulated and measured pressure traces are well matched during the combustion phase, where the kinetics play a major role, the results should not be significantly affected by the minor discrepancies caused by approximations of the geometry.

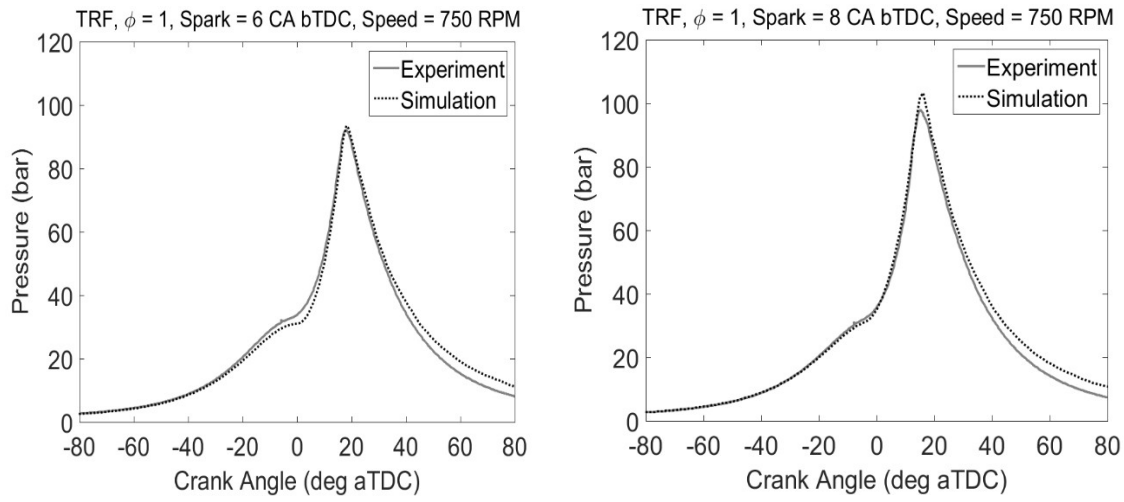

(a) (b)

Figure 2. Comparison of experimental and simulated pressure trace for TRF (a) 6 °CA bTDC (b) 8 °CA bTDC.

Engine experiments show that gasoline exhibits low temperature heat release (LTHR), intermediate temperature heat release (ITHR) and high temperature heat release (HTHR) depending on operating conditions.[44-46] Figure 3 presents the predicted unburned gas temperature history superimposed upon the simulated heat release profile for spark advances of 6 and 8 °CA bTDC. A two-stage ignition feature which is common to hydrocarbon fuels, and which was also observed in our RCM study[10] for gasoline and TRF under certain conditions, is predicted by the mechanism. NTC behaviour is also captured which is consistent with the ignition delay profiles of the TRF fuel observed in the RCM[10], but in this case it is indicated by the sharp decrease in heat release rate as temperature slightly increases. The first stage ignition represents the start of low temperature (cool flame) heat release and occurs after the induction period (period of slow oxidation) measured from TDC. For spark timings of 6 and 8 °CA bTDC, the first stage ignition occurred at 14.5 °CA aTDC and 10 °CA aTDC respectively at around T = 800 K, while the maximum first stage heat release occurred at 17 °CA aTDC and 13 °CA aTDC respectively. The earlier start of the first stage ignition at the spark timing of 8 °CA bTDC is due to the higher unburned gas temperatures obtainable at the higher spark advance of 8 °CA bTDC compared to 6 °CA bTDC. According to Pekalski et al.,[47] outside the NTC region an increase in the temperature of the end gas leads to a decrease in the induction period as well as an increase in the magnitude of the cool flame (i.e. heat release) mainly due to the disappearance of the peroxy radicals that drive the low temperature chemistry.

During the low temperature heat release, low temperature hydrocarbon oxidation reactions dominate and the gasoline fuel mixture is partially oxidised to form a large variety of stable and fairly stable intermediate products including alkenes, oxygenated molecular intermediates (e.g alcohols, aldehydes and ketones), water, oxides of carbon etc. These are not strongly exothermic reactions and thus a small amount of heat release results.[38, 47, 48] Reactions involving further oxidation of the partially oxidised fuel and oxidation of formed oxygenated compounds also occur during the low temperature heat release - the rates of these reactions increase with increasing pressure and temperature giving rise to higher heat release as seen in Figure 3b.

Fundamentally, the mechanism for the complete oxidation of hydrocarbon fuels begins by first of all initiation reactions involving H abstraction reactions by O_2 ($RH + O_2 = R. + HO_2$) and then mainly by OH radicals resulting in the formation of alkyl radicals. The alkyl radicals then react with oxygen to form the peroxy radical, RO_2. The alkyl/alkyl peroxy equilibrium is very significant in autoignition chemistry as the direction of the reaction at different temperature regimes determines to a large extent what chemistry would follow or become dominant.

Because of the negligible activation energy for the forward rate of $R + O_2 = RO_2$, at low temperatures, RO_2 is increasingly formed and further undergoes isomerisation to QOOH. QOOH in a second O_2 addition reaction can then combine with oxygen to promote chain-branching pathways[49] that result in the occurrence of a cool flame. A brute force sensitivity analysis of the current mechanism was carried out for ignition delay times in an RCM by Agbro et al.[10] Such an approach requires an additional simulation for each parameter under investigation, and hence, is prohibitively expensive from a computational point of view for a complex kinetic scheme within a stochastic engine simulation. However, such an analysis in a high pressure RCM across a range of temperatures can provide information of relevance here. The study of Agbro et al.[10] demonstrated that the low temperature chemistry for the TRF surrogate used here is dominated by H abstraction from *n*-heptane and iso-octane as well as to a lesser extent, the subsequent isomerisation of the peroxy radicals to QOOH species.

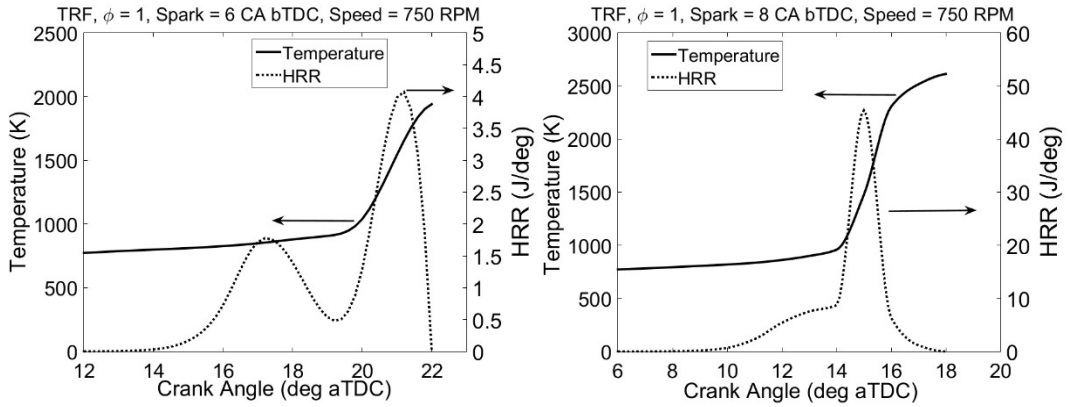

(a) (b)

Figure 3. Heat release rate (HRR) and temperature histories in the unburned zone simulated for TRF mixture (a) 6 °CA bTDC (b) 8 °CA bTDC.

As shown in Figure 4 only a small amount of the fuel (TRF) is consumed during the period of low temperature heat release, with a lower gradient in fuel loss for all three fuel components in this region compared to that seen at later times. OH radical concentrations are small in this region since OH reacts with the remaining fuel, but Figure 4 shows a small indistinct OH peak at the lower crank angles, in the region of low temperature heat release. The net heat release in the first stage ignition raises the temperature of the unburned gas and as a result, the average compressed gas temperature attained is greater than that resulting from adiabatic compression alone. With an increase in temperature, the equilibrium of $R + O_2 = RO_2$ now shifts towards the reactants. In addition, other inhibiting pathways become important, such as $R+O_2$ reacting to form HO_2 and conjugated alkenes, and QOOH decomposition. These pathways dominate over the low-temperature chain branching sequence, thus creating the lower reactivity typical of the negative temperature coefficient (NTC) region.[49] Competing unimolecular decomposition reactions via beta scission of QOOH or formation of cyclic ethers now begin to play a prominent role with an attendant decrease in reactivity, since they compete with the chain branching pathways which result from the second O_2 addition. For parent fuels which are alkanes, the decomposition of QOOH can, depending on the abstraction site, lead to the formation of an alkene + HO_2, a cyclic ether + OH, as well as an alkene + carbonyl radical.[50] HO_2 can also be formed via concerted elimination reactions involving RO_2. The NTC behaviour which is typical of alkanes now sets in due to a decrease in reactivity and results in a decrease in heat release as shown by the deepening of the heat

release curve at the locations between 13 CA and 14 °CA aTDC for the spark timing of 8 °CA bTDC (Figure 5a) and between 15 °CA aTDC and 17 °CA aTDC for the spark timing of 6 °CA bTDC (Figure 5b). Interestingly, as shown in Figure 6 for the spark timing of 8 °CA bTDC, we observe from the simulated species concentrations in the unburned zone that most of the alkyl peroxy radicals peak at slightly above 12 °CA aTDC and decrease in the NTC region thus providing an explanation for the suppression of reactivity and also the observed reduction in heat release at higher temperatures. The HO_2 formed during the NTC phase is however consumed in the combination reactions of HO_2 ($HO_2 + HO_2 = H_2O_2 + O_2$) and propagating reactions of HO_2 ($HO_2 + RH = H_2O_2 + R$) leading to the formation of H_2O_2. During the NTC stage there is a noticeable sharp rise in the production of formaldehyde (CH_2O) and hydrogen peroxide (H_2O_2) (Figure 5) which is consistent with the ignition delay sensitivity analysis performed in Agbro et al.[10] at 858 K where the formation of H_2O_2 from HO_2 dominates.

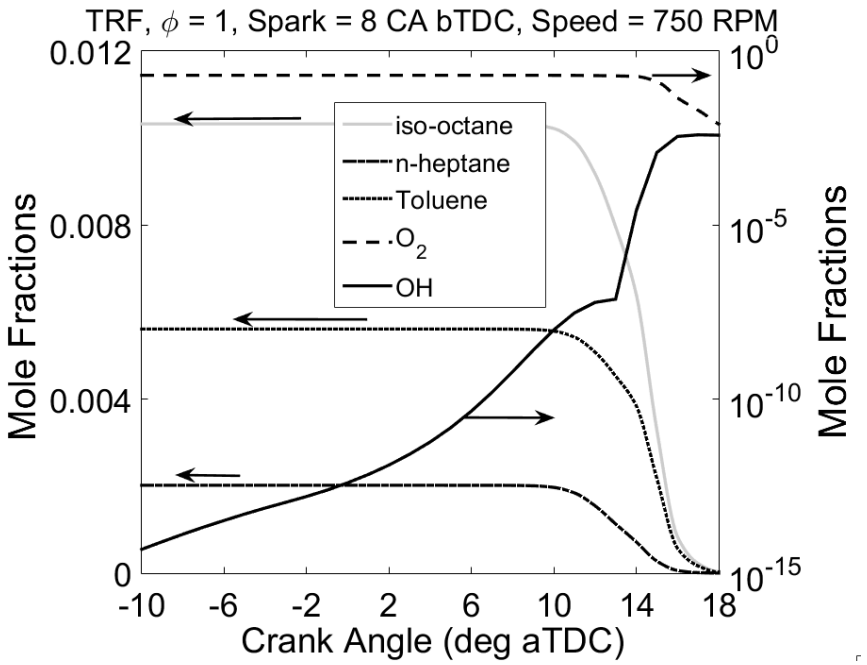

Figure 4. Simulated species concentrations of the reactants for the TRF mixture and OH histories in the unburned zone.

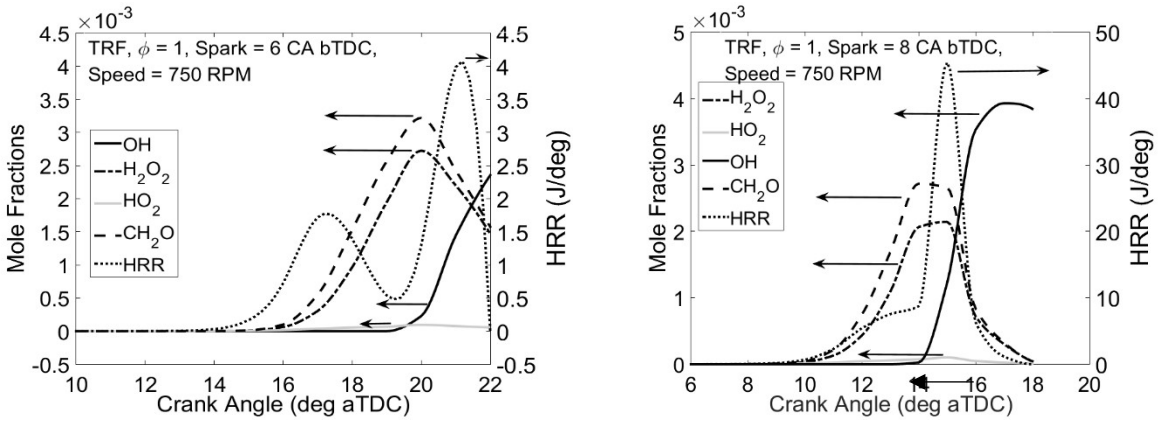

Figure 5. Rate of heat release in the unburned zone and species concentrations simulated for TRF mixture (a) 6 °CA bTDC (b) 8 °CA bTDC.

We also observe from Figure 6 that the concentrations of alkyl peroxy radicals (RO_2) peak before the concentrations of CH_2O and HO_2 reach their maximum. In addition, benzyl peroxy radicals are formed at earlier crank angles more than the alkyl peroxy radicals formed from n-heptane and iso-octane. Within the scheme, the formation of the benzyl peroxy radical from the benzyl radical through O_2 addition has a negative temperature dependence, and hence its formation is favoured over the alkyl peroxy radicals at the lower temperatures corresponding to crank angles before top dead centre. Its concentration then dips below other peroxy radicals at the later crank angles.

HO_2 and CH_2O are increasingly favoured at later crank angles and peak later than the alkyl peroxy radicals. The formation of both HO_2 and CH_2O involves a number of routes, many of which involve smaller C_1-C_4 molecules. An example of the main pathways demonstrated by an H atom flux analysis is included in the Supplementary Material for a constant volume stoichiometric simulation at 803 K and 30 bar. A major pathway for CH_2O formation is via CH_3O_2 both directly and via CH_3O. HO_2 is also formed from CH_3O, as well as from H, HCO, C_2H_5, CH_2OH and from the tert-butyl peroxy radical. The latter route was highlighted in the ignition delay sensitivity study of Agbro et al.[10] as an important reaction inhibiting reactivity at temperatures around the NTC region. The main loss for HO_2 is (as discussed above) the formation of H_2O_2. At higher temperatures, the H_2O_2 formed during the low temperature heat release is consumed in a decomposition reaction forming OH radicals. The formed OH radicals are responsible for the rapid consumption of the fuel at high temperatures in chain branching reactions in which more and more OH radicals are generated in the process. The

chemistry of H_2O_2 is responsible for the main stage ignition and high temperature heat release leading to the occurrence of knock.

The NTC phase predicted at a spark timing of 8 °CA bTDC (Figure 5b) is flatter and narrower compared to that predicted at a spark timing of 6 °CA bTDC (Figure 5a) and this can be attributed to the higher prevailing in-cylinder *P-T* conditions at 8 °CA aTDC that result in a higher heat release and consequently higher maximum temperature of the end gas. With higher end gas temperatures, high temperature reactions involving the decomposition of H_2O_2 (H_2O_2 (+M) = 2OH) are favoured over unimolecular QOOH decomposition and termination reactions and the main stage ignition occurs much earlier resulting in a smaller predicted NTC region as well as shorter predicted knock onset.

It should be noted at this point that the occurrence of a first stage ignition in the engine has serious implications in the sense that pre-conditioning of the air-fuel mixture (end gas) by the first stage heat release can lead to a reduction in the subsequent time required for the knock related second stage ignition to occur.[51, 52] Since the overall impact of the presence of a low temperature hydrocarbon oxidation (first-stage heat release) in an engine under the studied conditions is likely to be the enhancement of knock, methods that could suppress or eliminate the first-stage low temperature reactions could therefore potentially help in controlling the occurrence and intensity of knock. The use of oxygenated fuels such as ethanol and butanol have been proposed as a viable strategy for achieving desired higher engine efficiencies and lower carbon footprint while at the same time avoiding knock. It was found in Westbrook and Pitz[53] that the knock propensity of a given fuel can be effectively altered by modifying the low temperature heat release through the application of blending fuels or additives. Since previous RCM studies[10] demonstrated that the addition of *n*-butanol to gasoline/TRF fuels reduces NTC behaviour we next explore the ability of the B20 blends to reduce knock under practical engine conditions.

According to Khan[9], the autoignition phenomenon can be linked to the build-up of critical intermediate species and is distinguishable from the resulting heat release and temperature rise or from the point where the species attain certain concentration levels. In previous studies,[37, 38, 54] the occurrence or onset of knock in the engine has been identified by the analysis of the unburned zone heat release rate and species profiles. A sharp rise in the second stage heat release rate and temperature of the unburned mixture is caused by the autoignition of the end gas and high temperature exothermic oxidation of intermediate fuel species such as

CO, C_2H_4 etc. as well as the various oxygenated intermediate products produced during the cool flame phase. From the heat release profiles shown for the unburned zone in Figure 5, the predicted knock onsets at spark timings of 6 and 8 °CA bTDC are 19 and 13.8 °CA aTDC respectively, while the maximum heat release occurs at locations of 21 and 15 °CA aTDC respectively. The point of rapid rise in heat release coincides well with the point of rapid rise in OH radical concentrations as expected during chain branching and leading to the rapid consumption of the parent fuel at high temperatures. According to Moxey[48], the hot flame ignition or chemistry is marked with a strong presence of OH radicals. Yang et al. [55] reported in their study the onset of aldehyde chemiluminescence during the cool flame stage (low temperature hydrocarbon chemistry) while hydroxide species were detected close to the end of the low temperature hydrocarbon chemistry. However the hydroxyl radical concentrations increased across the main heat release stage. It is also clear from Figure 5 that hydrogen peroxide (H_2O_2) peaks near the point of hot ignition. The dominance of the chain branching step involving the decomposition reaction of H_2O_2 (H_2O_2 (+M) = 2 OH) at high temperatures is responsible for the consumption and decrease in the mole fractions of H_2O_2 during the main heat release stage.[48]

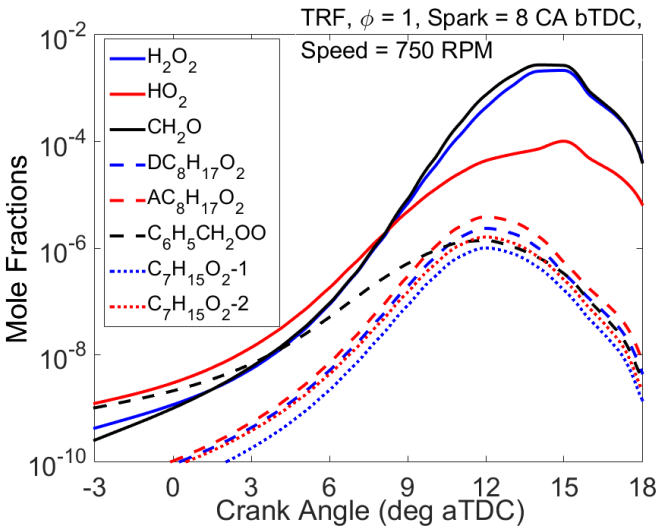

Figure 6. Simulated species concentrations of selected peroxy radicals in the unburned zone for TRF.

Figure 7 shows how the predicted knock onsets of TRF compare with the experimental knock onsets across spark timings of 6 - 8 °CA aTDC. Based on the experimental data, the formulated TRF provides a good representation of the behaviour of the reference gasoline at the earlier spark timings but some differences remain at later spark timings. The knock onsets

predicted by the TRF/*n*-butanol blended mechanism using the formulated TRF are consistently higher than the measured TRF knock onsets with the discrepancy again being more pronounced at the later spark timing of 6 °CA bTDC. Within the RCM[10], the autoignition delay times of TRF predicted by the mechanism across the range of temperatures investigated were also higher compared to the measured data. We also observe in Figure 7 that the disparity between the simulated and measured knock onsets decreases as the spark timing is advanced indicating that the mechanism performs better under higher in-cylinder *P*-*T* conditions where the dominant reactions are less related to the specific fuel molecule related chemistry as discussed above and in the previous RCM study.[10] It was shown previously in Figure 2 that the low temperature chemistry, in which the mechanism's performance is most deficient, is more dominant at the later spark timing than at the earlier spark timing (i.e. at higher in-cylinder *P*-*T* conditions) and this explains why the agreement of the predicted knock onset with the measured data is poorest at the later spark timing.

Based on the sensitivity study in Agbro et al.[10], the chemistry in the low temperature and NTC region is dominated by H abstraction by OH from the α, β and γ sites of iso-octane (labelled as a, b, c, within the mechanism included in supplementary material). The α, β and γ refer to 1º, 2 º, 3 º hydrogens respectively as shown in Figure 1 of Curran et al.,[50] with H abstraction from the α and β sites promoting reactivity and that from the γ site reducing reactivity. The latter is a main route for producing tert-butyl radicals which can go on to form HO_2 as discussed above. *n*-Heptane has only 1º and 2 º hydrogens with abstraction by OH leading to four different alkyl radicals. The RCM study of Agbro et al.[10] showed sensitivity to three of these with all of them promoting reactivity. The decomposition of hydrogen peroxide (H_2O_2 (+M) = OH + OH (+M)) was also seen to be important for promoting reactivity within the NTC. Further fundamental studies focused on reducing uncertainties in the rates of these reactions may help to improve agreement of the model with the measured data. The sensitivity study also highlighted a surprisingly high influence of the reaction toluene + OH = phenol + CH_3 compared to the expected hydrogen abstraction channel toluene + OH = $C_6H_5CH_2$ + H_2O on ignition delay predictions. Further probing showed that the toluene + OH channel leading to the formation of phenol + CH_3 was not updated along with other recent updates of the toluene + OH reaction pathways in the LLNL scheme.[56] It was also demonstrated in Agbro[57] that updating the current parameterisation of the reaction toluene + OH = phenol + CH_3 in the mechanism with the data from a recent study by Seta at al.[58] led to significant improvement in the predicted ignition delay times within the RCM. Therefore,

knock onset simulations were also performed within the engine framework using the rate constant from Seta et al.[58] for this reaction for comparison purposes.

Figure 7 shows that the knock onsets predicted using this updated rate constant are significantly shorter for TRF than those predicted by the original mechanism and lead to improvement in the agreement between the measured and predicted data across the spark timings investigated. Overall, qualitatively, the kinetic model captures the decrease in knock onsets observed in the measured data as spark timing is advanced similar to the experimental results presented in Agbro[57] and in the companion experimental paper. This suggests a certain confidence in the fidelity of the scheme based on its mechanistic structure and indicates that it could be used to a reasonable degree for knock onset prediction of TRF fuels within certain operating regimes of the SI the engine. Overall the mechanism and the formulated TRF performed best at the earlier spark timings where the impact of knock is more significant and where chemical kinetic modelling of fuels is of higher relevance. There are clearly further challenges in terms of improving the surrogate mechanism for predicting behaviour at the earlier spark timings. This is somewhat consistent with the ignition delay comparisons made in the parallel RCM study where the largest discrepancies between the gasoline and the TRF surrogate were at the lowest temperatures studied; below 740 K. Small discrepancies within the simulated pressures/temperatures following the optimisation process as discussed at the beginning of this section, may also affect the progress of the low temperature chemistry.

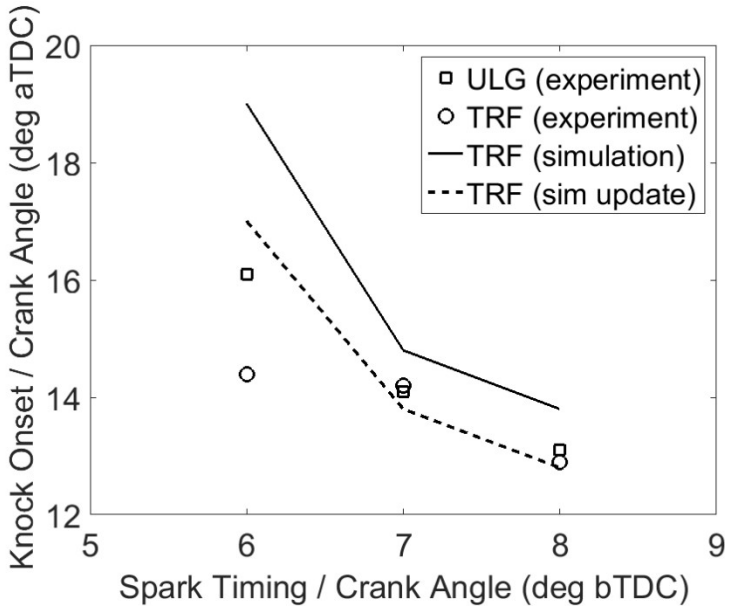

Figure 7. Predicted knock onsets of TRF using the updated mechanism in comparison with the knock onsets predicted by the original scheme and the experimental knock onsets for gasoline and TRF.

3.1.2 Prediction of the influence of *n*-butanol blending on the average knocking combustion properties of gasoline

Figures 8a and 8b show comparisons of the experimental and simulated pressure traces for the stoichiometric 20% by volume *n*-butanol/TRF blend at spark timings of 6 and 8 °CA bTDC respectively under in-cylinder conditions of 1.6 bar and 320 K. Figure 9 shows the equivalent predicted heat release and temperature profiles of the unburned zone. Similar to the results for TRF (Figure 2), the simulated pressure traces match the experimental pressure traces very closely except for after a crank angle of 35 °aTDC where the simulated pressure trace deviates from the measured trace, caused mainly by the approximated cylinder profile. Figure 9 shows that the kinetic model captures the influence of *n*-butanol blending on gasoline as demonstrated by the suppression and smoothening out of the cool flame/NTC region compared to that of TRF. In the ignition delay modelling in Agbro et al.[10] it was also observed that the NTC region for gasoline/TRF was suppressed due to the influence of *n*-butanol chemistry. Autoignition or knock will occur in an engine when the end gas, which is under additional compression and heating by the spark-initiated propagating flame, is unable to delay or resist autoignition before it is completely consumed by the advancing flame front. Therefore, fuel mixtures with longer delays are more likely to avoid the occurrence of knock. In the early stages of the compression phase of the end gas, very slow reactions occur leading to the production of a radical pool (i.e. OH radicals) that promotes the low temperature cool flame chemistry and consequently the occurrence of knock. In the previous section it was noted that fuels that inhibit the cool flame ignition have the potential to eliminate or reduce the impact of knock. That *n*-butanol exerts an inhibiting influence on the cool flame heat release of gasoline by scavenging of OH radicals produced during the induction phase[10] is apparent from Figure 9a but the impact diminishes at the higher spark advance (8 °CA bTDC) where the end gas temperatures are higher (Figure 9b). The sensitivity analysis carried out in Agbro et al.[10] suggests that the main reaction influencing the ignition delay times at lower temperatures for the blend is the H abstraction by OH from the α site of *n*-butanol leading to termination and competing with branching routes where OH abstracts an H from n-heptane, iso-octane and γ site of *n*-butanol.

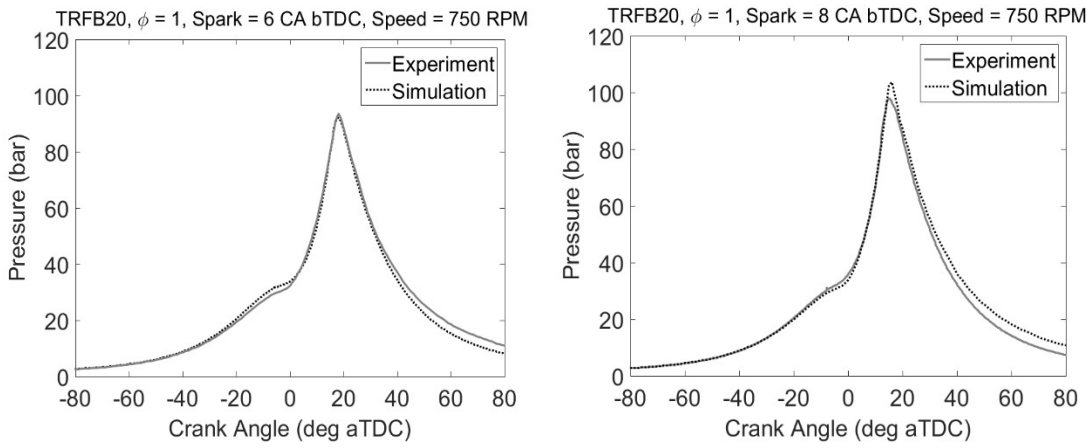

(a) (b)

Figure 8. Comparison of experimental and simulated pressure trace for TRF/*n*-butanol blend (a) 6 °CA bTDC (b) 8 °CA bTDC.

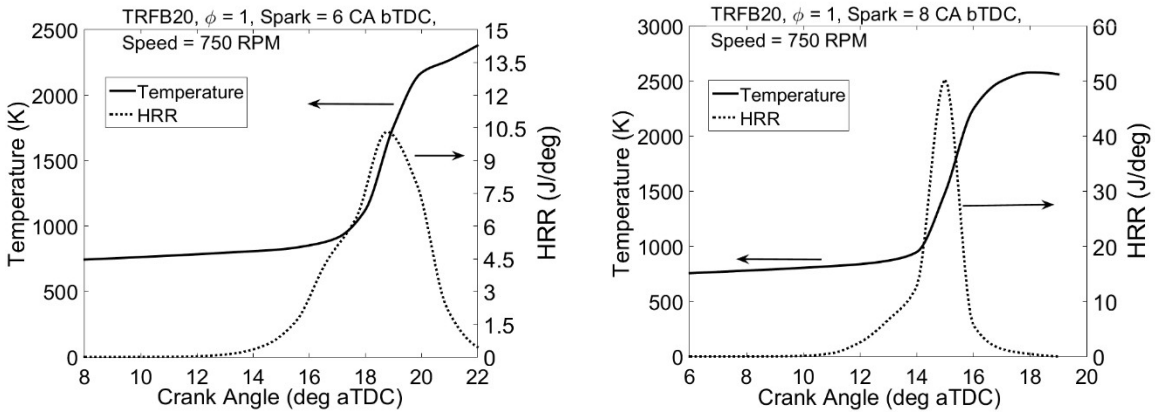

(a) (b)

Figure 9. Rate of heat release and temperature histories in the unburned zone simulated for TRF/*n*-butanol blend (a) 6 °CA bTDC (b) 8 °CA bTDC.

The predicted autoignition onset of the end gas for the TRF/*n*-butanol mixture given by the location of the sharp rise in OH and heat release rate (Figure 10) at spark timing of 6 and 8 °CA aTDC are 18 and 13.6 °CA aTDC respectively. The knock onsets of the TRF/*n*-butanol blend predicted by the mechanism are slightly lower than those predicted for TRF- the knock onsets predicted by the scheme across all the fuels investigated including neat *n*-butanol are presented and further discussed in the concluding part of this section. In Figure 10, similar to what was observed between the predicted knock onsets of TRF and TRF/*n*-butanol, the predicted peak concentrations of key species such as hydrogen peroxide (H_2O_2), formaldehyde (CH_2O) and OH for the TRF/*n*-butanol mixture are also slightly lower than

those predicted for TRF (Figure 5) confirming that the concentrations of the above key species are closely linked to the autoignition of the end gas. In both Figures 3 and 9 for TRF and TRF/*n*-butanol respectively, we observe that the prevalent engine temperatures predicted in the modelling work prior to the main stage autoignition (T = 920-980 K) are higher than the highest temperature attained in the RCM. Therefore, at a spark timing of 8 °CA bTDC, the differences between the predicted knock onset (autoignition delay) for TRF and TRF/*n*-butanol blend in the engine are quite small since as was observed in the RCM ignition delay data,[10] the impact of *n*-butanol blending on gasoline diminishes significantly as temperature is increased.

For the TRF/*n*-butanol blend, the predicted species concentration profiles of the alkyl peroxy radicals in the unburned zone at 8 °CA bTDC (Figure 11) peak at 13 °CA aTDC as against 12 °CA aTDC in the case of TRF. The slightly prolonged dominance of the chain branching reactions in the low temperature heat release phase of the TRF/*n*-butanol blend is responsible for the slightly lower knock onset predicted for the blend compared to TRF.

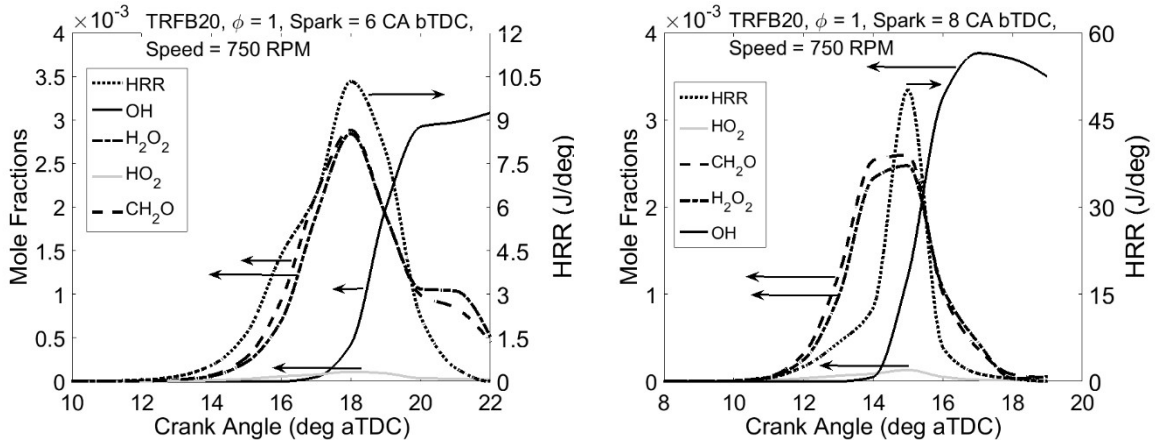

Figure 10. Heat release rate (HRR) in the unburned zone and species concentrations simulated for TRF/*n*-butanol blend (a) 6 CA bTDC (b) 8 CA bTDC.

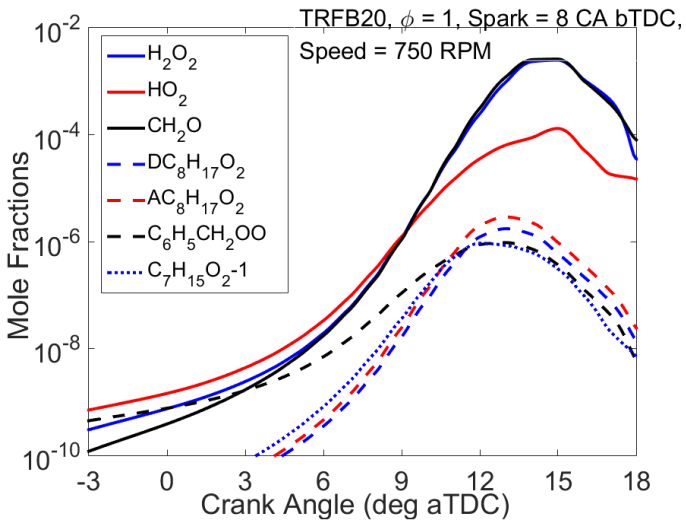

Figure 11. Simulated species concentrations of some peroxy radicals in the unburned zone for TRFB20.

Figure 12 shows how the predicted mean knock onsets for TRF/*n*-butanol compare with the measured mean knock onset across spark timings of 6-8 °CA bTDC. Again, similar to the results obtained for TRF, the predicted knock onsets for the TRF/ *n*-butanol blend are delayed compared to the measured knock onsets and the discrepancy is also highest at the later spark timing of 6 °CA bTDC. Figure 12 also shows that the near linear inverse relationship between the measured knock onsets and spark advance is also well replicated by the mechanism. Updates to the toluene reaction discussed above lead to lower predicted onsets than those predicted by the original scheme across the spark timing tested. However, the agreement with the measured data is only significantly improved at the earlier spark timing.

In the sensitivity analysis carried out within the RCM[10] for predicted TRF/*n*-butanol ignition delay times, the *n*-butanol + OH abstraction reaction from the γ site was found to be the most significant reaction influencing the predicted ignition delay times of TRF/*n*-butanol at higher temperatures (T = 858 K) with a reasonable contribution also coming from the abstraction reaction from the α site. The reactions of $HO_2 + HO_2 = H_2O_2 + O_2$ and H_2O_2 (+M) = 2 OH were also identified to be equally as important as the abstraction reaction from the γ site. It is worth mentioning that the uncertainties in the parameterisation of the rates of these reactions, particularly the uncertainties in the relative rates of *n*-butanol + OH abstraction reaction from the α and γ site were identified in Agbro et al.[59] to be very important for autoignition prediction in the temperature of interest. Therefore a more accurate quantification of the

branching ratio could lead to significant improvement in the robustness and accuracy of the scheme across the temperatures prevalent in the engine particularly at the later spark timing.

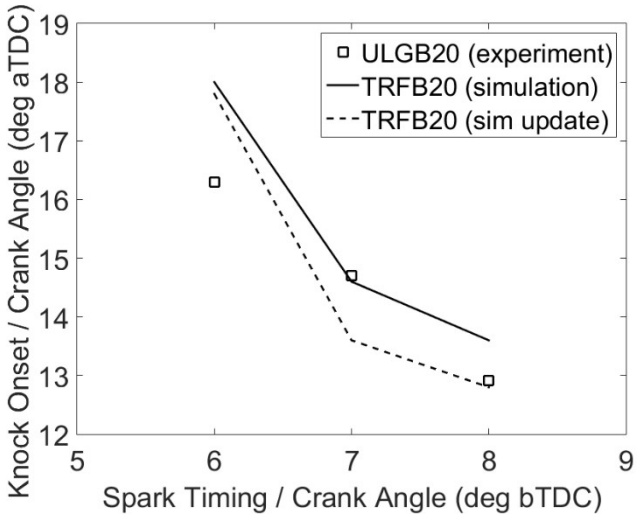

Figure 12. Predicted knock onsets of TRF/*n*-butanol blend using the updated mechanism in comparison with the knock onsets predicted by the original scheme and the experimental knock onsets for TRF/*n*-butanol blend.

Although engine experiments were not performed for pure *n*-butanol, the modelling of the autoignition onset of a pure *n*-butanol mixture was also carried out in this work using the same initial conditions based on the reference pressure data of gasoline in order to explore the potential of the mechanism in reproducing the lower ignition delay times predicted for *n*-butanol in the RCM at high temperatures compared to the TRF and TRF/*n*-butanol blend. Figure 13 shows a comparison of the predicted pressure profiles of stoichiometric *n*-butanol and the measured pressure data of reference gasoline while Figure 14 shows the predicted heat release profile of the unburned zone superimposed upon the temperature history of the unburned end gas, indicating the lack of a two stage heat release for pure *n*-butanol. The result showing the variation of the predicted knock onsets of *n*-butanol with spark timing is presented alongside those of TRF, TFRB20 and their measured data in Figure 15.

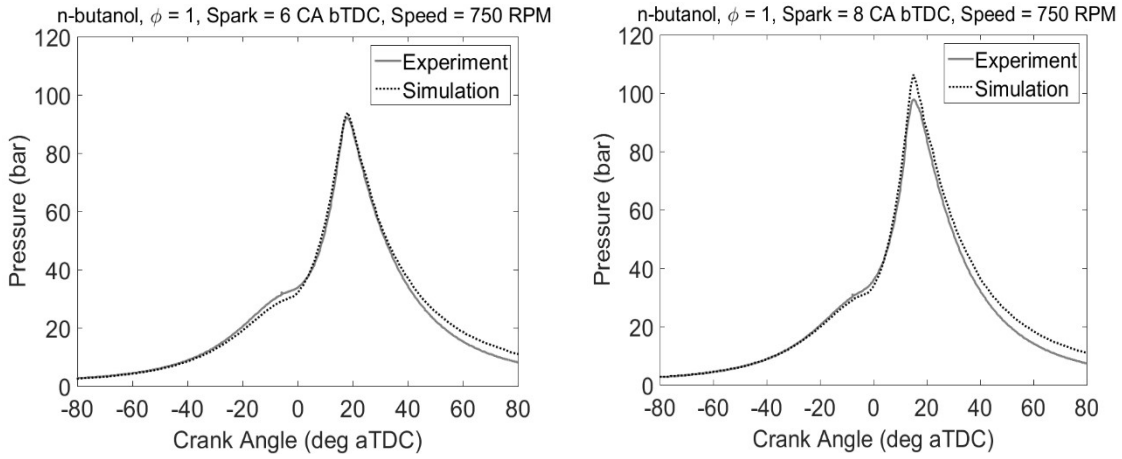

(a) (b)

Figure 13. Comparison of experimental and simulated pressure trace for *n*-butanol (a) 6 °CA bTDC (b) 8 °CA bTDC.

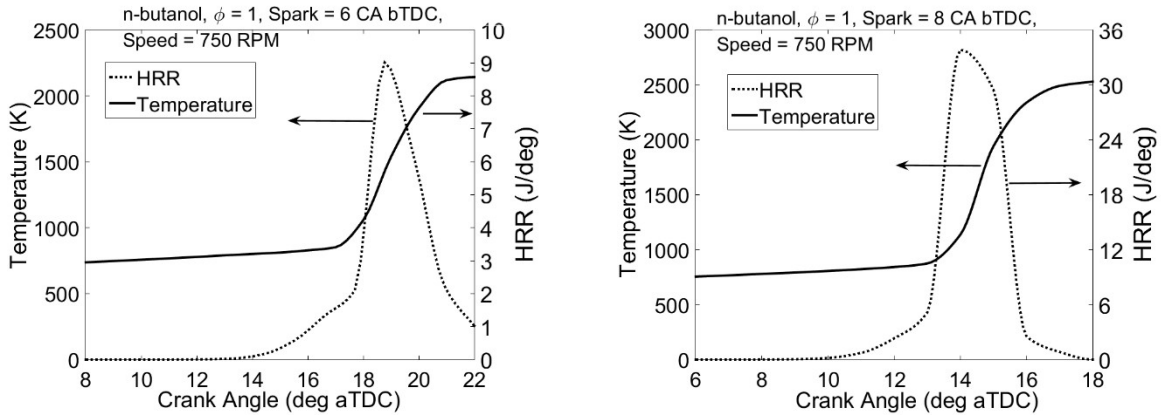

(a) (b)

Figure 14. Heat release rate (HRR) and temperature histories in the unburned zone simulated for *n*-butanol (a) 6 °CA bTDC (b) 8 °CA bTDC.

Figure 15 shows that the knock onset predictions are lowest for *n*-butanol across the spark timing tested and consistent with the predictions in the RCM at high temperatures.[10] While the TRF/*n*-butanol blended mechanism reproduces the trend between the measured knock onsets of TRF and the gasoline/ *n*-butanol blend at the earlier spark timing of 8 °CA bTDC, at the later spark timing of 6 °CA bTDC, the prediction of the influence of *n*-butanol on the knock onset of TRF is less good. This result is however in agreement with the observation in the RCM modelling work[10] where the predicted ignition delays for the TRF/*n*-butanol blend

were significantly lower than those predicted for TRF within the NTC region and at slightly higher temperatures.

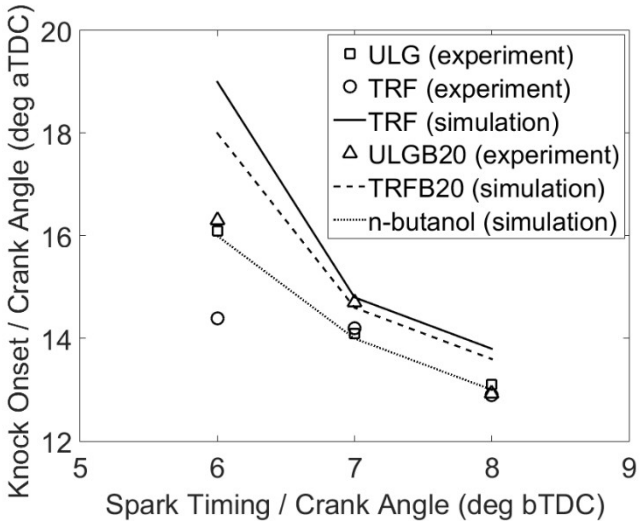

Figure 15. Comparison of predicted and measured knock onsets of TRF blended with 20 % *n*-butanol by volume with those of TRF, gasoline and *n*-butanol.

Overall, while the mechanism does not accurately reproduce the influence of *n*-butanol blending on gasoline as seen in the measured data at the later spark timing of 6 °CA bTDC, by comparing with the results obtained within the RCM[10], we observe that the performance of the mechanism is quite consistent across both set ups. This supports the view that for a chemical kinetic mechanism to correctly predict the autoignition characteristics of any fuel under practical engine conditions, it is crucial that the mechanism be able to accurately reproduce the ignition delay times at the temperature and pressure conditions seen in simpler set ups such as RCMs, particularly at conditions leading up to those prevalent in the engine. This point was also emphasised in Khan[9] where the ignition delay times predicted by the Golovitchev mechanism were consistently lower for iso-octane and TRF in both the engine and constant volume simulations within the NTC region.

4.0 Conclusions

In this work, the capacity of a reduced TRF/*n*-butanol mechanism in predicting the impact of *n*-butanol blending on gasoline combustion has been investigated under the framework of autoignition and knock modelling. The experimental measurement of knock onsets and knock

intensities carried out in the Leeds SI engine under boosted conditions for stoichiometric fuel/air mixtures at initial temperature and pressure conditions of 320 K and 1.6 bar respectively for a range of spark timings (2 °CA- 8 °CA bTDC) was used for the validation of the modelling work as well as for advancing the understanding of the influence of *n*-butanol on the knocking behaviour of gasoline. Similar to previous results obtained in an RCM[10], the knock onsets predicted for TRF and TRF/*n*-butanol blends under engine conditions were consistently higher than the measured data obtained from the Leeds engine. An update of the toluene + OH = phenol + CH_3 in the channels in the reduced TRF/*n*-butanol mechanism with recent data from Seta et al.[58] led to improvement in the agreement between the measured and predicted data for stoichiometric TRF mixtures across the spark timing investigated. For TRF/*n*-butanol mixtures, the agreement of the knock onsets predicted using the updated mechanism with the measured data was only significantly improved at the earlier spark timing of 8 °CA bTDC.

In conclusion, the work showed that for a chemical kinetic mechanism to correctly predict the autoignition and knock behaviour of any fuel under practical engine conditions, it is important that the mechanism also reproduce the autoignition delay times at the temperature and pressure conditions occurring in the RCM, i.e. *P*-*T* conditions approaching those that occur in the end gas of an SI engine. Thus, as accurate representation of the low-intermediate temperature chemistry in current chemical kinetic models of alternative fuels is very crucial for the accurate description of the chemical processes and autoignition of the end gas in the engine.

Acknowledgements

The authors would like to thank COST (European Cooperation in Science and Technology www.cost.eu) for providing financial support for scientific exchange visits to LOGE Lund Combustion Engineering under the COST Action SMARTCATs (CM 1404). We also thank Inna Gorbatenko for valuable discussions and contributions. We also wish to acknowledge the Tertiary Education Trust Fund (TETFUND), Nigeria, for scholarship funding for E. Agbro. The work at King Abdullah University of Science and Technology (KAUST) was funded under the Clean Combustion Research Center (CCRC) Future Fuels program.

References

1. Kalghatgi, G., Developments in internal combustion engines and implications for combustion science and future transport fuels. *Proceedings of the Combustion Institute* **2015,** 35, (1), 101-115.

2. AlRamadan, A. S.; Badra, J.; Javed, T.; Al-Abbad, M.; Bokhumseen, N.; Gaillard, P.; Babiker, H.; Farooq, A.; Sarathy, S. M., Mixed butanols addition to gasoline surrogates: Shock tube ignition delay time measurements and chemical kinetic modeling. *Combustion and Flame* **2015,** 162, (10), 3971-3979.

3. Douaud, A. M.; Eyzat, P., Four-Octane-Number Method for Predicting the Anti-Knock Behavior of Fuels and Engines. SAE Technical Paper: 780080, 1978.4.

4. Livengood, J. C.; Wu, P. C., Correlation of autoignition phenomena in internal combustion engines and rapid compression machines. *Symposium (International) on Combustion* **1955,** 5, (1), 347-356.

5. Halstead, M. P.; Kirsch, L. J.; Quinn, C. P., The autoignition of hydrocarbon fuels at high temperatures and pressures—Fitting of a mathematical model. *Combustion and Flame* **1977,** 30, 45-60.

6. Hu, H.; Keck, J. Autoignition of adiabatically compressed combustible gas mixtures; 0148-7191; SAE technical paper: 1987.

7. Liu, Z. Chemical Kinetics Modelling Study on Fuel Autoignition in Internal Combustion Engines. PhD Thesis, Loughborough University, 2010.

8. Liu, Z.; Chen, R., A zero-dimensional combustion model with reduced kinetics for SI engine knock simulation. *Combustion Science and Technology* **2009,** 181, (6), 828-852.

9. Khan, A. F. Chemical Kinetics Modelling of Combustion Processes in SI Engines. PhD Thesis, The University of Leeds, 2014.

10. Agbro, E.; Tomlin, A. S.; Lawes, M.; Park, S.; Sarathy, S. M., The influence of n-butanol blending on the ignition delay times of gasoline and its surrogate at high pressures. *Fuel* **2017,** 187, 211-219.

11. Yang, B.; Oßwald, P.; Li, Y.; Wang, J.; Wei, L.; Tian, Z.; Qi, F.; Kohse-Höinghaus, K., Identification of combustion intermediates in isomeric fuel-rich premixed butanol–oxygen flames at low pressure. *Combustion and flame* **2007,** 148, (4), 198-209.

12. Dagaut, P.; Sarathy, S. M.; Thomson, M. J., A chemical kinetic study of n-butanol oxidation at elevated pressure in a jet stirred reactor. *Proceedings of the Combustion Institute* **2009,** 32, (1), 229-237.

13. Sarathy, S.; Thomson, M.; Togbé, C.; Dagaut, P.; Halter, F.; Mounaim-Rousselle, C., An experimental and kinetic modeling study of *n*-butanol combustion. *Combustion and Flame* **2009,** 156, (4), 852-864.

14. Black, G.; Curran, H. J.; Pichon, S.; Simmie, J. M.; Zhukov, V., Bio-butanol: Combustion properties and detailed chemical kinetic model. *Combustion and Flame* **2010,** 157, (2), 363-373.

15. Moss, J. T.; Berkowitz, A. M.; Oehlschlaeger, M. A.; Biet, J.; Warth, V.; Glaude, P.-A.; Battin-Leclerc, F., An experimental and kinetic modeling study of the oxidation of the four isomers of butanol. *The Journal of Physical Chemistry A* **2008,** 112, (43), 10843-10855.

16. Grana, R.; Frassoldati, A.; Faravelli, T.; Niemann, U.; Ranzi, E.; Seiser, R.; Cattolica, R.; Seshadri, K., An experimental and kinetic modeling study of combustion of isomers of butanol. *Combustion and Flame* **2010,** 157, (11), 2137-2154.

17. Harper, M. R.; Van Geem, K. M.; Pyl, S. P.; Marin, G. B.; Green, W. H., Comprehensive reaction mechanism for n-butanol pyrolysis and combustion. *Combustion and Flame* **2011,** 158, (1), 16-41.

18. Sarathy, S. M.; Oßwald, P.; Hansen, N.; Kohse-Höinghaus, K., Alcohol combustion chemistry. *Progress in Energy and Combustion Science* **2014,** 44, 40-102.

19. Sarathy, S. M.; Farooq, A.; Kalghatgi, G. T., Recent progress in gasoline surrogate fuels. *Progress in Energy and Combustion Science* **2018,** 65, 67-108.

20. Pelucchi, M.; Bissoli, M.; Rizzo, C.; Zhang, Y.; Somers, K.; Frassoldati, A.; Curran, H.; Faravelli, T., A Kinetic Modelling Study of Alcohols Operating Regimes in a HCCI Engine. *SAE International Journal of Engines* **2017,** 10, (5), 2354-2370.

21. Walker, R. W., Morley, C., Basic Chemistry of Combustion. In *Comprehensive Chemical Kinetics: Low-temperature Combustion and Autoignition*, Pilling, M. J., Ed. Elsevier: 1997; Vol. 35.

22. Cox, R. A.; Cole, J. A., Chemical aspects of the autoignition of hydrocarbon□air mixtures. *Combustion and Flame* **1985,** 60, (2), 109-123.

23. Benson, S. W., The kinetics and thermochemistry of chemical oxidation with application to combustion and flames. *Progress in Energy and Combustion Science* **1981,** 7, (2), 125-134.

24. Chun, K. M.; Heywood, J. B.; Keck, J. C., Prediction of knock occurrence in a spark-ignition engine. *Symposium (International) on Combustion* **1989,** 22, (1), 455-463.

25. Cowart, J. S.; Keck, J. C.; Heywood, J. B.; Westbrook, C. K.; Pitz, W. J., Engine knock predictions using a fully-detailed and a reduced chemical kinetic mechanism. *Symposium (International) on Combustion* **1991,** 23, (1), 1055-1062.

26. Nishiwaki, K.; Yoshihara, Y.; Saijyo, K. *Numerical analysis of the location of knock initiation in SI engines*; 0148-7191; SAE Technical Paper: 2000.

27. Curran, H. J.; Pitz, W. J.; Westbrook, C. K.; Callahan, G. V.; Dryer, F. L., Oxidation of automotive primary reference fuels at elevated pressures. *Symposium (International) on Combustion* **1998,** 27, (1), 379-387.

28. Andrae, J. C. G.; Head, R. A., HCCI experiments with gasoline surrogate fuels modeled by a semidetailed chemical kinetic model. *Combustion and Flame* **2009,** 156, (4), 842-851.

29. Huang, C.; Golovitchev, V.; Lipatnikov, A., Chemical Model of Gasoline-Ethanol Blends for Internal Combustion Engine Applications. SAE Technical paper; 2010-01-0543, 2010.

30. Ra, Y.; Reitz, R. D., A combustion model for IC engine combustion simulations with multi-component fuels. *Combustion and Flame* **2011,** 158, (1), 69-90.

31. Lu, T.; Plomer, M.; Luo, Z.; Sarathy, S. M.; Pitz, W. J.; Som, S.; Longman, a. D. E., Directed relation graph with expert knowledge for skeletal mechanism reduction. In *The 7th US National Combustion Meeting*, Atlanta, GA, 2011., 2011.

32. Roberts, P. a. S., C., The Influence of Residual Gas NO Content on Knock Onset of Iso-Octane, PRF, TRF and ULG Mixtures in SI Engines. *SAE Int. J. Engines* **2013,** 6, (4), 2028-2043.

33. Konig, G.; Sheppard, C. *End gas autoignition and knock in a spark ignition engine*; 0148-7191; SAE Technical Paper 0148-7191: 1990.

34. LOGE_AB *LOGEengine v1.0, software manuals* http://www.logesoft.com, 2017.

35. Pasternak, M.; Netzer, C.; Mauss, F.; Fischer, M.; Sens, M.; Riess, M. In *Simulation of the Effects of Spark Timing and External EGR on Gasoline Combustion Under Knock-Limited Operation at High Speed and Load*, Cham, 2018; Springer International Publishing: Cham, 2018; pp 121-142.

36. Peters, N., *Turbulent combustion*. Cambridge Univeristy Press: 2000.

37. Pasternak, M.; Mauss, F.; Xavier, F.; Rieß, M.; Sens, M.; Benz, A., 0D/3D Simulations of Combustion in Gasoline Engines Operated with Multiple Spark Plug Technology. SAE Technical paper; 2015-01-1243, 2015.

38. Pasternak, M.; Mauss, F.; Sens, M.; Riess, M.; Benz, A.; Stapf, K. G., Gasoline engine simulations using zero-dimensional spark ignition stochastic reactor model and three-dimensional computational fluid dynamics engine model. *International Journal of Engine Research* **2015,** 17, (1), 76-85.

39. Bjerkborn, S. P., C; Fröjd, K; Mauss, F., Predictive Flame Propagation Model for Stochastic Reactor Model Based Engine Simulations. In *International Colloquium on the Dynamics of Explosions and Reactive Systems (ICDERS)*, California, USA., 2011.

40. Ling, Z. Flame Propagation and Autoignition in a High Pressure Optical Engine. PhD Thesis, The University of Leeds, 2014.

41. Hussein, A. M. T. New and Renewable Energy: Renewable Fuels in Internal Combustion Engines. PhD Thesis, The Univeristy of Leeds, 2012.

42. Materego, M. Auto-ignition Characterisation of Synthetic Fuels via Rapid Compression Machine. PhD Thesis, The University of Leeds, 2015.

43. Ahmed, A.; Hantouche, M.; Khurshid, M.; Mohamed, S. Y.; Nasir, E. F.; Farooq, A.; Roberts, W. L.; Knio, O. M.; Sarathy, S. M., Impact of thermodynamic properties and heat

loss on ignition of transportation fuels in rapid compression machines. *Fuel* **2018,** 218, 203-212.

44. Mehl, M.; J. Pitz, W.; Sjöberg, M.; E. Dec, J., Detailed Kinetic Modeling of Low-Temperature Heat Release for PRF Fuels in an HCCI Engine. SAE Technical Paper 2009-01-1806, 2009.

45. Kukkadapu, G.; Kumar, K.; Sung, C.-J.; Mehl, M.; Pitz, W. J., Autoignition of gasoline and its surrogates in a rapid compression machine. *Proceedings of the Combustion Institute* **2013,** 34, (1), 345-352.

46. Wolk, B.; Chen, J. Y.; Dec, J. E., Computational study of the pressure dependence of sequential auto-ignition for partial fuel stratification with gasoline. *Proceedings of the Combustion Institute* **2015,** 35, 2993-3000.

47. Pekalski, A. A.; Zevenbergen, J. F.; Pasman, H. J.; Lemkowitz, S. M.; Dahoe, A. E.; Scarlett, B., The relation of cool flames and auto-ignition phenomena to process safety at elevated pressure and temperature. *Journal of Hazardous Materials* **2002,** 93, (1), 93-105.

48. Moxey, B. G. A Study Of Flame Development with Iso-octane Alcohol Engine Blended Fuels in an Optical Spark Ignition Engine. PhD Thesis, Brunel University London, 2014.

49. Battin-Leclerc, F., Detailed chemical kinetic models for the low-temperature combustion of hydrocarbons with application to gasoline and diesel fuel surrogates. *Progress in Energy and Combustion Science* **2008**, 34, 440-498.

50. Curran, H. J.; Gaffuri, P.; Pitz, W. J.; Westbrook, C. K., A comprehensive modeling study of iso-octane oxidation. *Combustion and Flame* **2002,** 129, (3), 253-280.

51. Zheng, X.; Lu, T.; Law, C.; Westbrook, C.; Curran, H., Experimental and computational study of nonpremixed ignition of dimethyl ether in counterflow. *Proceedings of the Combustion Institute* **2005,** 30, (1), 1101-1109.

52. Mohamed, C. Autoigntion of Hydrocarbons in Relation to Knock. PhD Thesis, The University of Leeds, 1997.

53. Westbrook, C. K.; Pitz, W. J., Detailed Kinetic Modeling of Autoignition Chemistry. SAE Technical Paper; 872107, 1987.

54. Mittal, G.; Chaos, M.; Sung, C.-J.; Dryer, F. L., Dimethyl ether autoignition in a rapid compression machine: Experiments and chemical kinetic modeling. *Fuel Processing Technology* **2008,** 89, (12), 1244-1254.

55. Yang, C.; Zhao, H.; Megaritis, T., In-Cylinder Studies of CAI Combustion with Negative Valve Overlap and Simultaneous Chemiluminescence Analysis. SAE Technical Paper; 2009-01-1103, 2009.

56. Mehl, M.; Pitz, W. J.; Westbrook, C. K.; Curran, H. J., Kinetic modeling of gasoline surrogate components and mixtures under engine conditions. *Proceedings of the Combustion Institute* **2011,** 33, (1), 193-200.

57. Agbro, E. Experimental and chemical kinetic modelling study on the combustion of alternative fuels in fundamental systems and practical engines. PhD Thesis, The University of Leeds, 2017.

58. Seta, T.; Nakajima, M.; Miyoshi, A., High-temperature reactions of OH radicals with benzene and toluene. *The Journal of Physical Chemistry A* **2006,** 110, (15), 5081-5090.

59. Agbro, E.; Tomlin, A. S., Low temperature oxidation of n-butanol: Key uncertainties and constraints in kinetics. *Fuel* **2017,** 207, 776-789.